THE ASTROPHYSICAL JOURNAL, 494:L103–L106, 1998 February 10
© 1998. The American Astronomical Society. All rights reserved. Printed in U.S.A.

INJECTION OF SHORT-LIVED ISOTOPES INTO THE PRESOLAR CLOUD

ALAN P. BOSS[1] AND PRUDENCE N. FOSTER[2,3]
Received 1997 October 10; accepted 1997 December 4; published 1998 January 19

ABSTRACT

The evidence for short-lived isotopes such as ^{26}Al and ^{41}Ca in meteorites requires their production either by irradiation in the solar nebula or by nucleosynthesis in a supernova or other evolved star. In the latter case, nucleosynthesis must be followed promptly by injection of the isotopes into the presolar cloud, a feat presumably accomplished by the same stellar outflow that transported the isotopes to the presolar cloud and possibly triggered its collapse. If their nucleosynthesis occurs deep within an unmixed star, the short-lived isotopes may lag far behind the leading edge of the stellar outflow, perhaps preventing their injection. However, we show that lagging isotopes can be injected into a collapsing protostar with an efficiency similar to that of material in the leading edge of the outflow, because fast-moving isotopes initially far behind (approximately a few parsecs) the leading edge impact and enter the cloud while the injection process is still underway. Isotope injection proceeds through Rayleigh-Taylor–like clumps in the shock-compressed target cloud.

Subject headings: hydrodynamics — ISM: kinematics and dynamics — shock waves — solar system: formation

1. INTRODUCTION

Short-lived isotopes were present at the time of crystallization of their host meteorite phases in the solar nebula. Refractory inclusions in the primitive Allende meteorite show evidence for the presence of undecayed ^{26}Al (Lee, Papanastassiou, & Wasserburg 1976), while similar inclusions in Efremovka show evidence for once-live ^{41}Ca (Srinivasan, Ulyanov, & Goswami 1994; Srinivasan et al. 1996). The matrix of Efremovka seems to exhibit evidence for undecayed ^{36}Cl (Murty, Goswami, & Shukolyukov 1997). The mean lifetimes of ^{41}Ca, ^{36}Cl, and ^{26}Al are 1.5×10^5, 4.3×10^5, and 1.1×10^6 yr, respectively. Evidence for the existence of other short-lived isotopes has been presented as well, namely, ^{60}Fe, ^{53}Mn, and ^{107}Pd, with mean lifetimes less than 10^7 yr. If these short-lived isotopes were created by stellar nucleosynthesis, such as in a core collapse supernova (Cameron et al. 1995; Cameron, Vanhala, & Höflich 1997), then no more than $\sim 10^6$ yr could have elapsed between the supernova and the incorporation of the isotopes into solids in the solar nebula. Such a remarkably short time interval suggests that the collapse of the presolar cloud may have been triggered by the same event that injected the short-lived isotopes (Cameron & Truran 1977; Boss 1995).

However, alternative explanations for the origin of the short-lived isotopes have also been offered. Clayton & Jin (1995a) suggested that the ^{26}Al was produced by irradiation of the presolar cloud by cosmic rays, primarily $^{16}O^+$ ions. Bateman, Parker, & Champagne (1996) pointed out that if the ^{26}Al was produced by oxygen cosmic rays, then a sizable fraction of the solar system's oxygen atoms must have come from these cosmic rays, perhaps an implausibly large fraction. Clayton & Jin (1995b) also proposed that the ^{26}Al was produced in the outer layers of the solar nebula by cosmic rays (protons, He^+ ions, or $^{16}O^+$ ions) coming from solar flares or the solar wind. Both Clayton & Jin (1995b) and Bateman et al. (1996) found that the latter scenario required a cosmic-ray luminosity that was an uncomfortably large fraction of the proto-Sun's bolometric luminosity.

Goswami, Marhas, & Sahijpal (1997) show that there is no possible combination of flux of energetic protons and alpha particles and irradiation times that could explain the abundances of both ^{41}Ca and ^{26}Al, which are found together in refractory inclusions. Acknowledging this fact, Shu et al. (1997) suggested that ^{3}He particles striking a layered protorefractory inclusion could yield the correct abundances of ^{41}Ca and ^{26}Al. The absence of cosmic-ray tracks in coarse-grain refractory inclusions (Goswami et al. 1997) is explained in the latter scenario by heating the protorefractory inclusions after irradiation, thereby erasing the tracks.

Mixed injection and irradiation scenarios have also been advanced. Wasserburg et al. (1995) found that an asymptotic giant branch (AGB) star could synthesize the solar system abundances of ^{26}Al, ^{41}Ca, and ^{60}Fe but not the ^{53}Mn, which would have to be synthesized in the solar nebula by proton bombardment.

Considering the variety of possibilities, the relative contributions of supernovae, AGB stars, and local irradiation to the synthesis of meteoritic short-lived isotopes remain highly uncertain (Wasserburg, Busso, & Gallino 1996).

In our previous studies, we have shown that stellar winds from distant supernovae or from nearby AGB stars could both trigger the collapse of the presolar cloud and inject an appreciable fraction of shock front matter into the collapsing cloud (Boss 1995; Foster & Boss 1996 and 1997, hereafter FB1 and FB2, respectively). However, it has been pointed out by D. D. Clayton (1997, private communication) that short-lived isotopes may reside not in the shock front itself, but much farther behind, and so may not be injected into the presolar cloud. In particular, supernova nucleosynthesis models show that ^{26}Al and ^{41}Ca are primarily produced in the innermost 5 $M_\odot$ of a 15 $M_\odot$ progenitor star, and in the innermost 9 $M_\odot$ of a 25 $M_\odot$ star (Woosley & Weaver 1995). In the absence of efficient mixing in the stellar interior or during the supernova explosion, then, these isotopes will lag far behind the leading edge of the supernova ejecta.

We address here the question of how far behind the shock front isotopes can lag and still be injected into the presolar cloud. If injection efficiencies are negligible for lagging iso-

[1] Department of Terrestrial Magnetism, Carnegie Institution of Washington, 5241 Broad Branch Road, NW, Washington, DC 20015-1305.
[2] Center for Climate Systems Research, University of Tokyo, 4-6-1 Komaba, Meguro-ku, Tokyo 153, Japan.
[3] Institute for Study of the Earth's Interior, Okayama University, Misasa, Tottori-ken 682-01, Japan.

topes, then stellar nucleosynthesis might have to be ruled out as the source of the solar system's short-lived isotopes.

2. NUMERICAL METHODS AND INITIAL MODELS

As in our previous work (FB1 and FB2), we present numerical calculations of the interaction of stellar shock fronts with target dense cloud cores, following in a single calculation both the process of shock compression and triggered collapse and the injection of shock front matter. We follow the location of the short-lived isotopes with two complementary techniques, Lagrangian tracers and a "color" equation identical to the continuity equation (FB2). The two techniques provide independent checks on the accuracy of our computed injection efficiencies. Compared with our previous work, which was restricted to tracers lying initially within the shock front, we consider here the trajectories of tracers initially within the shock front as well as far behind it ("lagging tracers").

The calculations were performed in two spatial dimensions with the VH-1 hydrodynamics code (Lindahl 1992), which is based on the "piecewise parabolic method" of Colella & Woodward (1984). The VH-1 code is third-order accurate in space and second-order accurate in time, and does an excellent job of resolving shock structures. The self-gravity of the target cloud was included by solving the Poisson equation as a boundary value problem (FB1).

The initial conditions for the shock front and target cloud were chosen to be the same as those for the standard case described in FB2. The cylindrical coordinate (r, z) grid was taken to be axisymmetric about the z-axis. The numerical grid extended from $z = +0.19$ to $z = -0.19$ pc for the model (LW = "lagging wind") with the greatest extent of lagging tracers, and from $r = 0$ to $r = 0.093$ pc. Grid spacings were uniform, with up to 240 zones in z and 60 zones in r (37 within the target cloud radius).

The incoming shock front propagates down the z-axis and strikes the target cloud, which is a stationary, 1 $M_\odot$ cloud located at the coordinate system's origin. The cloud initially had a central density $\rho_c = 6.2 \times 10^{-19}$ g cm^{-3}, a radius of 0.058 pc, and the density profile of the critically stable, isothermal (10 K) Bonnor-Ebert sphere. The number density and temperature of the intercloud medium were set at 10^3 cm^{-3} and 10 K, respectively. The shock front consisted of a planar pulse of momentum with a density of 10^4 cm^{-3}, a temperature of 10 K, and a thickness of 0.0031 pc in the z-direction, moving at 20 km s^{-1} toward the cloud.

The only significant change from the standard case of FB2 was with regard to the wind velocity—we define the "wind" to be the region upstream of the shock front. The wind had a density of 10^2 cm^{-3} and a temperature of 10 K, as in FB2 and model LS ("lagging standard"), but a velocity of 20 km s^{-1} in model LW, the same as the shock front. In contrast, the FB2 standard case and model LS both had an initially stationary wind that is unlikely to be conducive to the injection of laggards. In fact, calculations of supernova remnants that have traversed a distance on the order of 10 pc show that the cool (10 K), dense shell of swept-up matter has a velocity of about 20 km s^{-1} and is followed by ejecta moving at a comparable or even higher velocity (Chevalier 1974), justifying our choices of 20 km s^{-1} for the shock and the wind velocities. However, the supernova wind is considerably hotter than 10 K (Chevalier 1974), an effect that we do not attempt to model here—isothermality at 10 K is assumed throughout this Letter. As discussed at length in FB2, the isothermal assumption appears to be reasonably accurate. In addition, models with hot shocks and hot winds led to increased injection efficiencies (FB2), so we believe we are being conservative by retaining the isothermal assumption here.

3. RESULTS

We present the results of two new models with variations in the initial distance of the tracers behind the shock front and in the wind velocity. The key quantity we calculate is the injection efficiency η (FB2), which we define to be the fraction of the incident mass (incoming matter with an initial impact parameter less than the radius of the cloud) that is injected into the collapsing protostar (within one zone or 0.0015 pc of the cloud's density maximum). Values are tabulated for both the color (η_c) and the tracers (η_t); $\eta_c \approx \eta_t$ implies a self-consistent solution.

The first model (LS) had zero wind velocity, the same as the standard model of FB2, and had tracers initially located not only within the shock front of thickness 0.0031 pc, but also within a zone extending two shock thicknesses upstream of the shock front. The lagging tracers were thus initially in a region with zero velocity. The tracers that were initially in the shock front were injected into the protostar with the same efficiency ($\eta_t = 0.16$) as found in FB2, as must be the case since adding passive tracers can have no effect on the hydrodynamics. The tracers that were located in the region immediately behind the shock front (up to one shock thickness behind) were injected with significantly lower efficiency, $\eta_t = 0.05$, while those located even farther behind (up to two shock thicknesses behind) were not injected at all ($\eta_t \approx 0$). The latter behavior can be understood as a result of the fact that the lagging tracers began with zero velocity and only began to move down the z-axis as a result of the development of a small pressure gradient after the shock front had departed and impacted the target cloud. By this time, the outermost, uncollapsed regions of the target cloud have begun to rebound outward (see Fig. 4 of FB2), preventing the injection of nearly all of the slow-moving, lagging tracers. Evidently with zero wind velocity, tracers lagging more than a single shock thickness behind the shock front cannot be injected.

The second model (LW) had a wind velocity of 20 km s^{-1}, and tracers and color fields initially located up to a distance of two cloud radii (0.12 pc) behind the shock front, a region 40 times larger than the shock front thickness. The color field was set to zero in the top five rows of cells, from $z = 0.182$ to 0.190 pc, in order to avoid the inflow of additional color during the evolution. We found that tracers from throughout the extended upstream region were injected into the protostar with roughly equal efficiencies; η_t ranged from about 0.066 to 0.080, with no clear trend being obvious (i.e., there was no hint that $\eta_t \rightarrow 0$ for larger initial values of z). Evidently, tracers at much greater distances behind the shock front will also be injected with similar efficiencies.

By the end of the calculation for model LW, at a time of 660,000 yr, the color and tracer injection efficiencies agreed reasonably well, with $\eta_t = 0.072$ and $\eta_c = 0.097$. Both of these values are considerably less than the efficiency of $\eta_t = 0.16$ found in model LS. This drop can be attributed to the deleterious effect of the high-speed wind in model LW: the 20 km s^{-1} wind ablates material off the outer edge of the shock-compressed cloud, stripping away target cloud, shock front, and wind material that is eventually injected by Rayleigh-Taylor–like fingers in the absence of the high-speed wind (FB2).

The high-speed wind simply shears off the upstream portions of the Rayleigh-Taylor (R-T) fingers. The high-speed wind also ablates significant target cloud matter: the final protostar contains only 0.5 $M_\odot$, compared with the initial cloud mass of 1 $M_\odot$, and compared with the final protostar mass of 0.8 $M_\odot$ in model LS.

We believe that the injection of lagging tracers is enabled by the nature of the injection process. FB2 found that R-T fingers appeared to provide the conduits for injecting shock front matter into the collapsing protostar. Tracer trajectory plots in FB2 show that bundles of tracers with similar initial radii (independent of z inside the shock front) were either injected together or rejected, with the deciding factor being whether or not they happened to enter a penetrating R-T finger in the shock-compressed region. Independence of initial z is much more evident in model LW (Fig. 1), where it can be seen that the trajectories of injected tracers starting with very different initial distances upstream from the shock front nevertheless are nearly identical.

Because the R-T fingers develop and exist over a good portion of the evolution (for about 200,000 yr), there is ample time for severely lagging tracers to catch up with their predecessors and be injected. In fact, tracers moving with the wind velocity of 20 km s^{-1} might then start as much as 4 pc *behind the shock front* and still be injected. While we have not tried to simulate injection directly from such great distances, we believe that this prediction is entirely consistent with our models and with our understanding of injection driven by R-T–like instabilities.

We note that the initially small size of the R-T clumps (see Fig. 6 of FB2) is consistent with a heuristic estimate of the fastest growing wavelength of the R-T instability, based upon the R-T analysis of Chandrasekhar (1961). Replacing the surface tension per unit length in the classic R-T analysis with the dimensionally equivalent gas pressure, which is the only restoring force in the present models, the fastest growing R-T wavelength can be expressed approximately as $\lambda_* \approx 2\pi 3^{1/2} Z\,(c_s/v_z)$, where Z is the thickness of the shock-compressed layer, c_s is the isothermal sound speed (0.2 km s^{-1}), and v_z is the shock speed (20 km s^{-1}). For model LW, λ_* is equal to $\approx 0.1Z$, a value consistent with the spacing of the clumps evident at 22,000 yr in Figure 6 of FB2. The clumps grow and merge together at later times, as gravitational collapse and injection proceeds.

4. DISCUSSION

Our models imply that isotopes being carried by a 20 km s^{-1} stellar wind could be injected into a shock-triggered, collapsing protostar, even starting from considerable (approximately a few parsecs) distances behind the shock front. The precise location of specific short-lived isotopes in the stellar outflow is somewhat uncertain, depending on factors such as the mass of the star and the amount of mixing before and after ejection from the star. However, our result that isotopes moving anywhere along a parsecs-long sector of a stellar outflow can still be injected makes the question of the precise location in the outflow, at most, of possible importance for the sequence of injection rather than for whether or not injection occurs.

In sufficiently massive presupernova stars, some fraction of the "ejected" mass may fall back onto the collapsed remnant rather than escape to infinity. For the 15 and 25 $M_\odot$ solar-composition stars considered by Woosley & Weaver (1995), a few tenths of a solar mass of initially ejected matter falls back,

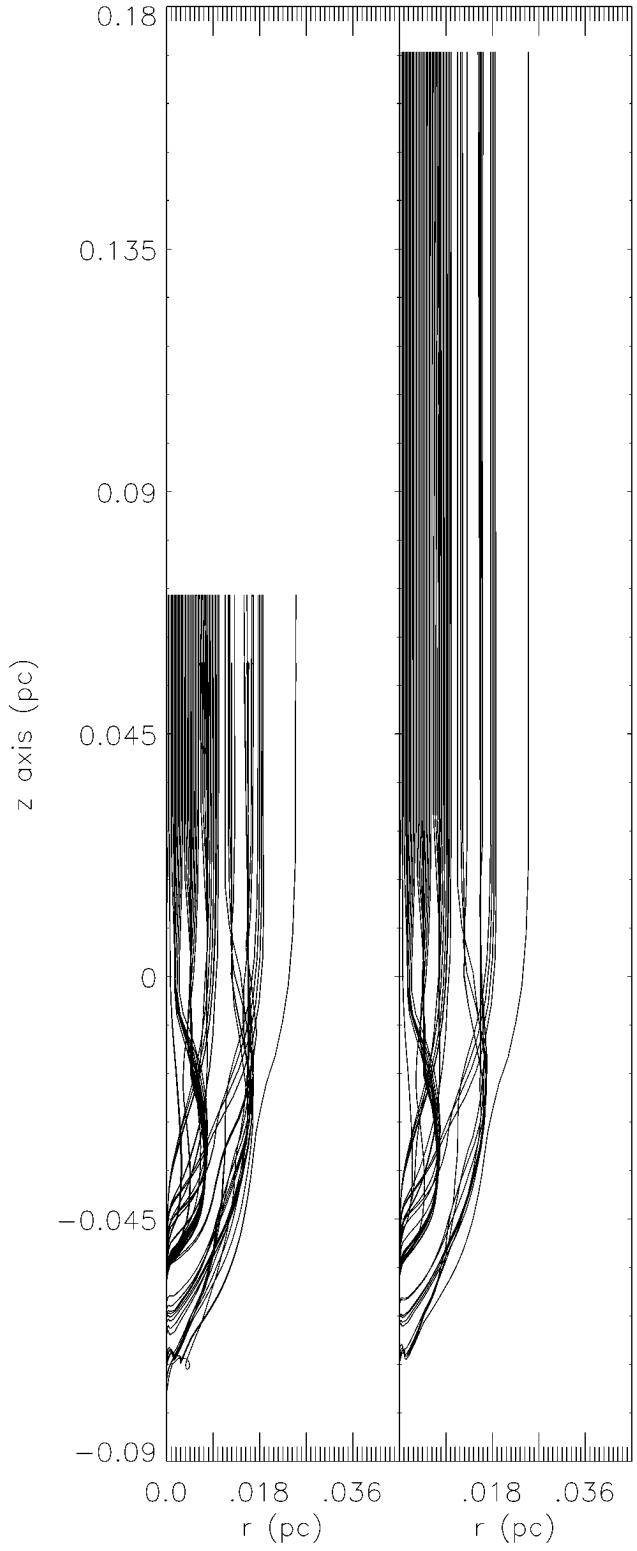


FIG. 1.—Trajectories for tracers that were injected into the model LW protostar, which forms along the symmetry (z) axis and then is accelerated downward. *Left*: tracers that were initially located from 0 to 0.014 pc behind the leading edge of the shock front. *Right*: tracers that were initially located from 0.10 to 0.12 pc behind the shock front. The trajectories are nearly identical, indicating that lagging tracers quickly overtake their predecessors, and that injection occurs nearly independently of the distance behind the shock front.

and the final masses of the collapsed remnants are 1.4 and 2.1 $M_\odot$, respectively. Because ^{26}Al and ^{41}Ca are synthesized exterior to these mass cuts, these short-lived isotopes should be completely ejected during the supernova explosion. The extent to which these isotopes are mixed into overlying matter during the supernova explosion and its subsequent expansion cannot be calculated in the spherically symmetrical models of Woosley & Weaver (1995) and remains to be determined (see, e.g., Arnett, Fryxell, & Müller 1989).

In a 25 $M_\odot$ star, ^{26}Al is produced in the hydrogen-burning shell and is mixed throughout the star's envelope by dredge-ups during the red giant phase (Woosley & Weaver 1995). However, this dredge-up mechanism does not work for ^{41}Ca in the 25 $M_\odot$ star, or for either ^{26}Al or ^{41}Ca in the 15 $M_\odot$ star, in which case these isotopes will be laggards.

Prior to undergoing supernova explosions, stars with masses in the range of 25–120 $M_\odot$ are Wolf-Rayet (WR) stars. WR stars lose mass at very high rates and thereby eject products of hydrogen and helium shell–burning. Arnould, Paulus, & Meynet (1997) found that WR stars with a range of masses would eject significant amounts of ^{26}Al, ^{36}Cl, ^{41}Ca, and ^{107}Pd, but insufficient ^{53}Mn and ^{60}Fe, which could only be synthesized during the subsequent supernova explosion. Short-lived isotopes produced during the WR phase would still be alive by the time that the WR star experiences the supernova explosion. In this case, the leading edge of the supernova front might contain short-lived isotopes from the earlier WR phase, followed by freshly synthesized laggards.

Finally, the present calculations assume isothermality. However, calculations of shock-triggered collapse using a smoothed particle hydrodynamics (SPH) code and variable adiabatic thermodynamics generally did not lead to injection for shocks that induced collapse (Cameron et al. 1997). More recently, H. Vanhala (1997, private communication) duplicated the standard (isothermal) case of FB2 with the SPH code and found an injection efficiency comparable to that of FB2. This suggests that variable adiabatic thermodynamics can prevent injection, whereas FB2 found that including nonisothermal shock and wind temperatures only increased injection efficiencies. The source of this possible discrepancy is under investigation.

5. CONCLUSIONS

We have used detailed numerical calculations of the interaction of stellar shock fronts with dense cloud cores to demonstrate that injection occurs even for lagging isotopes, with an injection efficiency of about 7%–10% in the relevant model (LW) examined here, the same as that for tracers initially within the shock front itself. While our numerical models prove that isotopes lagging as far as 0.12 pc behind the shock front are injected with undiminished efficiency, we argue that laggards as far as several parsecs behind the leading edge of the shock front will still be injected. This is true for the following reason: the laggards move at high speeds that allow them to overtake their predecessors, which have been decelerated in the shock-compressed cloud. Those laggards that happen to strike R-T–like fingers will be injected into the protostar over a time period of ~200,000 yr.

Our result alleviates the suspicion that short-lived isotopes synthesized deep within a supernova, e.g., might somehow avoid being injected into the dense cloud cores encountered by the expanding supernova remnant. As a consequence, the stellar nucleosynthesis and injection scenario for explaining the origin of the solar system's short-lived isotopes remains worthy of attention.

We thank Donald D. Clayton for raising the issue of lagging isotopes, and Harri Vanhala and A. G. W. Cameron for discussions. The calculations were performed on the DEC Alpha workstations of the Carnegie Institution of Washington. A. P. B. was partially supported by NASA Planetary Geology and Geophysics grant NAG5-3873, and P. N. F. by grants from the M. J. Walter Foundation and the Japanese Society for the Promotion of Science. This research was also supported by NASA Origins of Solar Systems grant NAG5-4306.

REFERENCES

Arnett, D., Fryxell, B., & Müller, E. 1989, ApJ, 341, L63
Arnould, M., Paulus, G., & Meynet, G. 1997, A&A, 321, 452
Bateman, N. P. T., Parker, P. D., & Champagne, A. E. 1996, ApJ, 472, L119
Boss, A. P. 1995, ApJ, 439, 224
Cameron, A. G. W., Höflich, P., Myers, P. C., & Clayton, D. D. 1995, ApJ, 447, L53
Cameron, A. G. W., & Truran, J. W. 1977, Icarus, 30, 447
Cameron, A. G. W., Vanhala, H., & Höflich, P. 1997, in Astrophysical Implications of the Laboratory Study of Presolar Materials, ed. T. J. Bernatowicz & E. Zinner (New York: AIP), 665
Chandrasekhar, S. 1961, Hydrodynamic and Hydromagnetic Stability (New York: Dover)
Chevalier, R. A. 1974, ApJ, 188, 501
Clayton, D. D., & Jin, L. 1995a, ApJ, 451, 681
———. 1995b, ApJ, 451, L87
Colella, P., & Woodward, P. R. 1984, J. Comput. Phys., 54, 174
Foster, P. N., & Boss, A. P. 1996, ApJ, 468, 784 (FB1)
Foster, P. N., & Boss, A. P. 1997, ApJ, 489, 346 (FB2)
Goswami, J. N., Marhas, K. K., & Sahijpal, S. 1997, in 28th Annu. Lunar Planet. Sci. Conf., March 17–21 (Houston: Lunar Planet. Inst.), 439
Lee, T., Papanastassiou, D. A., & Wasserburg, G. J. 1976, Geophys. Res. Lett., 3, 41
Lindahl, G. 1992, Master's thesis, Univ. Virginia
Murty, S. V. S., Goswami, J. N., & Shukolyukov, Yu. A. 1997, ApJ, 475, L65
Shu, F. H., Shang, H., Glassgold, A. E., & Lee, T. 1997, Science, 277, 1475
Srinivasan, G., Sahijpal, S., Ulyanov, A. A., & Goswami, J. N. 1996, Geochim. Cosmochim. Acta, 60, 1823
Srinivasan, G., Ulyanov, A. A., & Goswami, J. N. 1994, ApJ, 431, L67
Wasserburg, G. J., Busso, M., & Gallino, R. 1996, ApJ, 466, L109
Wasserburg, G. J., Gallino, R., Busso, M., Goswami, J. N., & Raiteri, C. M. 1995, ApJ, 440, L101
Woosley, S. E., & Weaver, T. A. 1995, ApJS, 101, 181